Biomedical Optics EXPRESS

Verification of the lack of correlation between age and longitudinal chromatic aberrations of the human eye from the visible to the infrared

Masashi Nakajima,[1,2] Takahiro Hiraoka,[3] Yoko Hirohara,[2] Tetsuro Oshika,[3] and Toshifumi Mihashi[1,*]

[1]*Department of Information Processing, Tokyo Institute of Technology, Kanagawa, 226-8503, Japan*
[2]*Development Engineering Dept., Eye Care Company, TOPCON, Tokyo, 174-8580, Japan*
[3]*Department of Ophthalmology, Institute of Clinical Medicine, University of Tsukuba, Ibaraki, 305-8575, Japan*
[*]*mihashi.t.aa@m.titech.ac.jp*

Abstract: Several researchers studied the longitudinal chromatic aberration (LCA) of the human eye and observed that it does not change due to age. We measured the LCA of 45 subjects' normal right eyes at three distinct wavelengths (561, 690, and 840 nm) using a Hartmann–Shack wavefront aberrometer (HSWA) while consecutively switching between three light sources for wavefront sensing. We confirmed that the LCA of the human eye does not change due to age between 22 and 57 years.

OCIS codes: (330.7325) Visual optics, metrology; (170.4460) Ophthalmic optics and devices; (330.5370) Physiological optics; (330.4875) Optics of physiological systems; (330.7326) Visual optics, modeling.

References and links

1. R. E. Bedford and G. Wyszecki, "Axial Chromatic Aberration of the Human Eye," J. Opt. Soc. Am. **47**(6), 564–565 (1957).
2. P. A. Howarth, "The lateral chromatic aberration of the eye," Ophthalmic Physiol. Opt. **4**(3), 223–226 (1984).
3. M. Rynders, B. Lidkea, W. Chisholm, and L. N. Thibos, "Statistical distribution of foveal transverse chromatic aberration, pupil centration, and angle psi in a population of young adult eyes," J. Opt. Soc. Am. A **12**(10), 2348–2357 (1995).
4. L. N. Thibos, A. Bradley, D. L. Still, X. Zhang, and P. A. Howarth, "Theory and measurement of ocular chromatic aberration," Vision Res. **30**(1), 33–49 (1990).
5. S. Marcos, S. A. Burns, P. M. Prieto, R. Navarro, and B. Baraibar, "Investigating sources of variability of monochromatic and transverse chromatic aberrations across eyes," Vision Res. **41**(28), 3861–3871 (2001).
6. R. Navarro, J. Santamaría, and J. Bescós, "Accommodation-dependent model of the human eye with aspherics," J. Opt. Soc. Am. A **2**(8), 1273–1281 (1985).
7. J. E. Kelly, T. Mihashi, and H. C. Howland, "Compensation of corneal horizontal/vertical astigmatism, lateral coma, and spherical aberration by internal optics of the eye," J. Vis. **4**(4), 262–271 (2004).
8. P. Artal, A. Benito, and J. Tabernero, "The human eye is an example of robust optical design," J. Vis. **6**(1), 1–7 (2006).
9. L. N. Thibos, A. Bradley, and X. X. Zhang, "Effect of ocular chromatic aberration on monocular visual performance," Optom. Vis. Sci. **68**(8), 599–607 (1991).
10. G. Wyszecki and W. S. Stiles, *Color Science* (Wiley Interscience Publication, 2000)
11. J. S. McLellan, S. Marcos, P. M. Prieto, and S. A. Burns, "Imperfect optics may be the eye's defence against chromatic blur," Nature **417**(6885), 174–176 (2002).
12. A. Dubra and Y. Sulai, "Reflective afocal broadband adaptive optics scanning ophthalmoscope," Biomed. Opt. Express **2**(6), 1757–1768 (2011).
13. G. Wald and D. R. Griffin, "The Change in Refractive Power of the Human Eye in Dim and Bright Light," J. Opt. Soc. Am. **37**(5), 321–336 (1947).
14. L. N. Thibos, M. Ye, X. Zhang, and A. Bradley, "The chromatic eye: a new reduced-eye model of ocular chromatic aberration in humans," Appl. Opt. **31**(19), 3594–3600 (1992).
15. S. Marcos, S. A. Burns, E. Moreno-Barriusop, and R. Navarro, "A new approach to the study of ocular chromatic aberrations," Vision Res. **39**(26), 4309–4323 (1999).
16. L. Llorente, L. Diaz-Santana, D. Lara-Saucedo, and S. Marcos, "Aberrations of the Human Eye in Visible and Near Infrared Illumination," Optom. Vis. Sci. **80**(1), 26–35 (2003).

#237205 Received 30 Mar 2015; revised 16 Jun 2015; accepted 17 Jun 2015; published 25 Jun 2015

17. W. N. Charman and J. A. Jennings, "Objective measurements of the longitudinal chromatic aberration of the human eye," Vision Res. **16**(9), 999–1005 (1976).
18. M. Vinas, C. Dorronsoro, D. Cortes, D. Pascual, and S. Marcos, "Longitudinal chromatic aberration of the human eye in the visible and near infrared from wavefront sensing, double-pass and psychophysics," Biomed. Opt. Express **6**(3), 948–962 (2015).
19. P. Artal, E. Berrio, A. Guirao, and P. Piers, "Contribution of the cornea and internal surfaces to the change of ocular aberrations with age," J. Opt. Soc. Am. A **19**(1), 137–143 (2002).
20. T. Fujikado, T. Kuroda, S. Ninomiya, N. Maeda, Y. Tano, T. Oshika, Y. Hirohara, and T. Mihashi, "Age-related changes in ocular and corneal aberrations," Am. J. Ophthalmol. **138**(1), 143–146 (2004).
21. I. Brunette, J. M. Bueno, M. Parent, H. Hamam, and P. Simonet, "Monochromatic Aberrations as a Function of Age, from Childhood to Advanced Age," Invest. Ophthalmol. Vis. Sci. **44**(12), 5438–5446 (2003).
22. T. Oshika, S. D. Klyce, R. A. Applegate, and H. C. Howland, "Changes in Corneal Wavefront Aberrations with Aging," Invest. Ophthalmol. Vis. Sci. **40**(7), 1351–1355 (1999).
23. A. Guirao, M. Redondo, and P. Artal, "Optical aberrations of the human cornea as a function of age," J. Opt. Soc. Am. A **17**(10), 1697–1702 (2000).
24. C. Ware, "Human axial chromatic aberration found not to decline with age," Graefes Arch. Clin. Exp. Ophthalmol. **218**(1), 39–41 (1982).
25. P. A. Howarth, X. X. Zhang, A. Bradley, D. L. Still, and L. N. Thibos, "Does the chromatic aberration of the eye vary with age?" J. Opt. Soc. Am. A **5**(12), 2087–2092 (1988).
26. M. Millodot, "The influence of age on the chronatic aberration of the eye," Albrecht Von Graefes Arch. Klin. Exp. Ophthalmol. **198**(3), 235–243 (1976).
27. J. A. Mordi and W. K. Adrian, "Influence of age on chromatic aberration of the human eye," Am. J. Optom. Physiol. Opt. **62**(12), 864–869 (1985).
28. S. Manzanera, C. Canovas, P. M. Prieto, and P. Artal, "A wavelength tunable wavefront sensor for the human eye," Opt. Express **16**(11), 7748–7755 (2008).
29. E. J. Fernández and P. Artal, "Ocular aberrations up to the infrared range: from 632.8 to 1070 nm," Opt. Express **16**(26), 21199–21208 (2008).
30. J. F. Castejón-Mochón, N. López-Gil, A. Benito, and P. Artal, "Ocular wave-front aberration statistics in a normal young population," Vision Res. **42**(13), 1611–1617 (2002).
31. J. Porter, A. Guirao, I. G. Cox, and D. R. Williams, "Monochromatic aberrations of the human eye in a large population," J. Opt. Soc. Am. A **18**(8), 1793–1803 (2001).
32. S. Koh, N. Maeda, T. Kuroda, Y. Hori, H. Watanabe, T. Fujikado, Y. Tano, Y. Hirohara, and T. Mihashi, "Effect of tear film break-up on higher-order aberrations measured with wavefront sensor," Am. J. Ophthalmol. **134**(1), 115–117 (2002).
33. S. Koh, N. Maeda, Y. Hirohara, T. Mihashi, S. Ninomiya, K. Bessho, H. Watanabe, T. Fujikado, and Y. Tano, "Serial Measurements of Higher-Order Aberrations After Blinking in Normal Subjects," Invest. Ophthalmol. Vis. Sci. **47**(8), 3318–3324 (2006).
34. L. N. Thibos, R. A. Applegate, J. T. Schwiegerling, and R. Webb; VSIA Standards Taskforce Members. Vision science and its applications, "Standards for reporting the optical aberrations of eyes," J. Refract. Surg. **18**(5), S652–S660 (2002).
35. L. N. Thibos, X. Hong, A. Bradley, and R. A. Applegate, "Accuracy and precision of objective refraction from wavefront aberrations," J. Vis. **4**(4), 329–351 (2004).
36. D. A. Atchison and G. Smith, "Chromatic dispersions of the ocular media of human eyes," J. Opt. Soc. Am. A **22**(1), 29–37 (2005).
37. J. H. Zar, *Biostatistical Analysis* (Prentice Hall 2010).
38. R Core Team, (2013). R: A language and environment for statistical computing. R Foundation for Statistical Computing, Vienna, Austria. URL *http://www.R-project.org/*.
39. N. López-Gil and P. Artal, "Comparison of double-pass estimates of the retinal-image quality obtained with green and near-infrared light," J. Opt. Soc. Am. A **14**(5), 961–971 (1997).
40. E. J. Fernández, A. Unterhuber, P. M. Prieto, B. Hermann, W. Drexler, and P. Artal, "Near infrared ocular wavefront sensing with a femtosecond laser," ARVO abstract 2836 (2004).
41. Y. Le Grand, *Form and Space Vision*, rev. ed., translated by M. Millodot and G. Heath (Indiana University Press, Bloomington, Ind., 1967)
42. J. E. Koretz, S. A. Strenk, L. M. Strenk, and J. L. Semmlow, "Scheimpflug and high-resolution magnetic resonance imaging of the anterior segment: a comparative study," J. Opt. Soc. Am. A **21**(3), 346–354 (2004).
43. M. Takehana and L. Takemoto, "Quantitation of membrane-associated crystallins from aging and cataractous human lenses," Invest. Ophthalmol. Vis. Sci. **28**(5), 780–784 (1987).
44. N. S. Malik, S. J. Moss, N. Ahmed, A. J. Furth, R. S. Wall, and K. M. Meek, "Ageing of the human corneal stroma: structural and biochemical changes," Biochim. Biophys. Acta **1138**(3), 222–228 (1992).
45. D. X. Hammer, G. D. Noojin, R. J. Thomas, D. J. Stolarski, B. A. Rockwell, and A. J. Welch, "Ocular Dispersion," Proc. SPIE 3591, Ophthalmic Technoloies IX **3291**, 22–32 (1999).
46. M. Dubbelman and G. L. Van der Heijde, "The shape of the aging human lens: curvature, equivalent refractive index and the lens paradox," Vision Res. **41**(14), 1867–1877 (2001).
47. D. A. Atchison, E. L. Markwell, S. Kasthurirangan, J. M. Pope, G. Smith, and P. G. Swann, "Age-related changes in optical and biometric characteristics of emmetropic eyes," J. Vis. **8**(4), 29 (2008).

#237205 Received 30 Mar 2015; revised 16 Jun 2015; accepted 17 Jun 2015; published 25 Jun 2015

48. A. Glasser and M. C. W. Campbell, "Presbyopia and the optical changes in the human crystalline lens with age," Vision Res. **38**(2), 209–229 (1998).
49. B. A. Moffat, D. A. Atchison, and J. M. Pope, "Age-related changes in refractive index distribution and power of the human lens as measured by magnetic resonance micro-imaging in vitro," Vision Res. **42**(13), 1683–1693 (2002).
50. R. H. H. Kröger, "Methods to estimate dispersion in vertebrate ocular media," J. Opt. Soc. Am. A **9**(9), 1486–1490 (1992).
51. J. S. Larsen, "The sagittal growth of the eye. II. Ultrasonic measurement of the axial diameter of the lens and the anterior segment from birth to puberty," Acta Ophthalmol. (Copenh.) **49**(3), 427–440 (1971).
52. D. O. Mutti, K. Zadnik, R. E. Fusaro, N. E. Friedman, R. I. Sholtz, and A. J. Adams, "Optical and structural development of the crystalline lens in childhood," Invest. Ophthalmol. Vis. Sci. **39**(1), 120–133 (1998).
53. T. Kuroda, T. Fujikado, N. Maeda, T. Oshika, Y. Hirohara, and T. Mihashi, "Wavefront analysis in eyes with nuclear or cortical cataract," Am. J. Ophthalmol. **134**(1), 1–9 (2002).
54. E. Fernández and W. Drexler, "Influence of ocular chromatic aberration and pupil size on transverse resolution in ophthalmic adaptive optics optical coherence tomography," Opt. Express **13**(20), 8184–8197 (2005).
55. I. Powell, "Lenses for correcting chromatic aberration of the eye," Appl. Opt. **20**(24), 4152–4155 (1981).
56. Y. Benny, S. Manzanera, P. M. Prieto, E. N. Ribak, and P. Artal, "Wide-angle chromatic aberration corrector for the human eye," J. Opt. Soc. Am. A **24**(6), 1538–1544 (2007).
57. R. J. Zawadzki, B. Cense, Y. Zhang, S. S. Choi, D. T. Miller, and J. S. Werner, "Ultrahigh-resolution optical coherence tomography with monochromatic and chromatic aberration correction," Opt. Express **16**(11), 8126–8143 (2008).
58. P. Pérez-Merino, C. Dorronsoro, L. Llorente, S. Durán, I. Jiménez-Alfaro, and S. Marcos, "In vivo chromatic aberration in eyes implanted with intraocular lenses," Invest. Ophthalmol. Vis. Sci. **54**(4), 2654–2661 (2013).

1. Introduction

The human eye has large chromatic aberrations. Chromatic aberrations are divided into three categories: longitudinal chromatic aberrations (LCA), transverse chromatic aberrations (TCA), and difference among higher-order aberrations (HOA) in several wavelengths. An LCA is defined as the difference between two focuses in two different wavelengths. A TCA is defined as the difference of image heights between two different wavelengths. For the optics of the eye, the focus is always near the cornea for short wavelengths and farther away for long ones, and when uncorrected this causes LCA [1]. Because the optics of the eye are not rotationally symmetrical, even for the vision in the fovea, misalignments between the ocular components and the off-axis position of the fovea result in TCA [2–5]. Although the eye has four refractive surfaces and four optical materials, and thus is more complicated than a standard achromatic doublet lens, the chromatic dispersions of the materials are too similar to compensate for LCA [6]. Interestingly, off-axis TCA theoretically does have a compensation mechanism because it is an asymmetrical aberration and coma, which is an asymmetrical aberration, is compensated for in the optics [7, 8].

A large LCA of over 2 diopters (D) in the visible region was found in several previous studies. But this does not directly cause deterioration of vision. The effect of the LCA on the polychromatic modulation transfer function (MTF) is approximately the same as that of a monochromatic MTF with 0.20 D defocus [9] because the spectral luminance sensitivity is limited by the spectral sensitivity of human vision [10], and monochromatic aberrations play a protective role by softening the influence of retinal blur derived from chromatic aberrations [11]. However, for objective measurements of the eye, the LCA is problematic. For adaptive optics (AO) in high-resolution retinal imaging, the LCA causes blurring and focus shifts at the retina. For this reason, the wavelength band of the AO system in one previous study was narrow (<10 nm in the visible region) [12].

We investigate individual differences in LCA during objective refraction in the range between near-infrared (NIR) wavelengths and the center point of the visible wavelengths. This is because most objective refractions are performed in the NIR range, while subjective refractions are performed at visible wavelengths. This discrepancy in refraction is compensated by bias constants in the instruments; manufacturers empirically determine the values of the required constants. If individual variations were observed in the LCA, the fixed bias value used for objective refractions would not be able to compensate for the LCA of at

#237205 Received 30 Mar 2015; revised 16 Jun 2015; accepted 17 Jun 2015; published 25 Jun 2015

least some subjects. Subjects with intraocular lenses (IOL) would encounter a discrepancy between the NIR and the visible different from that in normal human eyes if the chromatic dispersion of IOLs was not the same as that of the crystalline lens.

Chromatic aberrations of the human eye have been studied by several researchers. Wald and Griffin [13] and Bedford and Wyszecki [1] reported that the LCA of the human eye is approximately 2 D in the visible region, adjusting the best focus point subjectively; the measurement wavelengths ranged from 365 to 750 nm and from 389 to 700 nm, and the studies examined 5 and 12 subjects, respectively. Thibos et al. [14] reported the same range, between 400 and 700 nm, with 8 subjects and using a two-color Vernier-alignment technique: the subject moves the Vernier target subjectively. Several objective methods were used for measuring the LCA. Marcos et al. [15] found that the LCA was 1.26 D in the visible region between 450 and 650 nm with 3 subjects, as measured by spatially resolved refractometer. Llorente et al. [16] reported that the average LCA between 543 nm and 787 nm was 0.72 D, as measured by two methods: one was a laser ray tracing with 25 eyes, and the other was a Hartmann-Shack wavefront aberrometer (HSWA) with 11 eyes. The discrepancies between the LCA values obtained using objective measurements and those obtained using both objective and subjective measurements were also investigated [17, 18]. Vinas et al. [18] recently integrated the double-pass, HSWA, and psychophysical measurements into an AO system and reported that while the objectively measured LCA values were identical, at 0.55 D between 555 and 700 nm, the psychophysically measured value was significantly larger.

The effect of age on monochromatic aberrations has been studied by several researchers using HSWAs. Artal et al. [19], Fujikado et al. [20], and Brunette et al. [21] used an HSWA, and they all reported that total ocular aberrations increased with aging. The measurements were taken in NIR wavelengths; the studies had 17, 66, and 114 subjects respectively; and the age ranges were 26 to 69, 4 to 69, and 5 to 82, respectively. In addition to HSWA measurements of ocular wavefront aberrations, Oshika et al. [22] and Guirao et al. [23] used a corneal topographer to investigate corneal aberrations across different age groups, and they found that corneal aberrations also increased with age.

Ocular chromatic aberrations associated with aging have been also studied. Ware [24] and Howarth et al. [25], who used Badal optometers, objectively observed that the LCA was not related to aging. They compared the results from younger and older groups of subjects; the measurement wavelengths ranged from 420 to 740 nm and from 420 to 645 nm; they examined 12 and 10 subjects; and the subjects' age ranges were 13 to 65 and 27 to 72, respectively. On the other hand, several researchers reported some change in connection with aging. Millodot [26] reported that the LCA between 458 and 656 nm decreased with age. The number of subjects in that study was 58; the subjects adjusted the best focus point subjectively. Mordi et al. [27] reported the same for the range between 437 and 671 nm, with 8 subjects using a Rodenstock-refractometer. Manzanera et al. [28] and Fernández and Artal [29] measured age-related changes in the LCA using an HSWA. Manzanera et al. studied three subjects; Fernández and Artal studied seven.

We chose HSWA as a method of investigating LCA. One reason is that this method has been proven to measure the objective refraction and monochromatic HOA accurately. Some researchers, including Castejón-Mochón et al. [30] and Porter et al. [31], have measured the monochromatic HOA of hundreds of eyes using this method. The other reason is that this method is independent of aberrations in the measurement instrument (unless both the aberrations to be measured and those of the instrument are large). This is because HS detects the difference in aberrations between the measured raw data and the reference. Thus, by beginning with the reference in each wavelength, we were able to accurately measure refractions and aberrations in multiple wavelengths using an instrument originally designed for use in other (NIR) wavelengths.

In the present study, we performed clinical measurements on 45 normal eyes, ranging in age from 22 to 57, using an HSWA with three light sources at different wavelengths. The

#237205 Received 30 Mar 2015; revised 16 Jun 2015; accepted 17 Jun 2015; published 25 Jun 2015

wavelengths used were 840, 690, and 561 nm. The HSWA was calibrated in these three wavelengths using a specially built reflective artificial eye containing a hyperbolic mirror. This eye is free of chromatic aberrations because the only power component is a mirror, and it is virtually free of monochromatic aberrations because the hyperbolic mirror is in an aberration-free condition. The aim of this research is to investigate individual differences in LCA with age, from the central visible wavelengths through to the NIR wavelengths, using a modern objective instrument to measure more eyes than the previous study with the same method. We investigated correlations between LCA and age, spherical equivalent (SE), and other biometrics of the eye, and the necessity of an adaptive compensation system to balance individual LCA differences in high-resolution retinal imaging.

2. Methods and analysis

2.1 Subjects and apparatus

We took measurements of the normal right eyes of 45 subjects under no cycloplegia. None of the eyes had any ocular abnormalities other than refractive errors. All of the participants were emmetropic or myopic, and their ages were 35.7 ± 11.5 years (range: 22–57). The numbers of subjects in their twenties, thirties, forties, and fifties respectively were 19, 7, 12, and 7. The SEs were −3.75 ± 2.21 D (range: −8.25 to −0.22). This study was approved by the Institutional Review Board at the Tsukuba University Hospital and adhered to the tenets of the Declaration of Helsinki

We developed an HSWA with three different light sources (Fig. 1). The basis of the HSWA was the same as in the previous studies [32, 33]. The HSWA was originally designed for the NIR wavefront sensing in 840 nm with a super-luminescent diode (SLD) as a light source. The lenslet array of the wavefront sensor consisted of 700 small lenses, with 0.2 mm spacing and 5 mm focal length, and a CCD (CS3910, Toshiba-Teli, Tokyo). The anterior part of the eye was observed during the wavefront sensing using 950 nm NIR light with the other CCD (BS-680PT, Texas Instruments, Inc., Texas). The same fixation target as that of a commercially available auto-refractometer (RM-8000, Topcon, Japan) was used. Commercially available auto-refractometers often have wavelengths of approximately 840 nm. For this study, we added other two light sources, with wavelengths of 561 and 690 nm. One of these, 561 nm, is near the peak of the spectral sensitivity of the human eye. The other, 690 nm, is roughly the midpoint between 561 and 840 nm. Three optical fibers from each light source were bundled together and closely aligned with each other in the same cladding. The structure of fibers compacted the apparatus enough that it could be used in the clinic. The end of each fiber was always placed conjugated with the fovea of the eye. The fibers, fixation target, and wavefront sensor were moved to adjust the spherical error of each subject (Fig. 1).

The refraction and chromatic aberration of the apparatus were calibrated using a reflective artificial eye that we built for this purpose. The artificial eye consists of an off-axis hyperbolic mirror and diffuser (Fig. 2). Theoretically, an infinite object along its optical axis will focus on the focal point of the mirror with no aberrations. There are few aberrations in images of axial objects that are not located at infinity, but the aberrations are small, less than 0.02 μm RMS for a defocus of −9 D. Between −9 and 0 D, this design provided not only a chromatic aberration-free optics but also an almost totally aberration-free optics (the RMS is less than λ/14). Although aberrations become larger as the incident angle to the artificial eye increases, the aberration-free condition remains as long as the angle is smaller than ± 0.5 degrees.

#237205 Received 30 Mar 2015; revised 16 Jun 2015; accepted 17 Jun 2015; published 25 Jun 2015

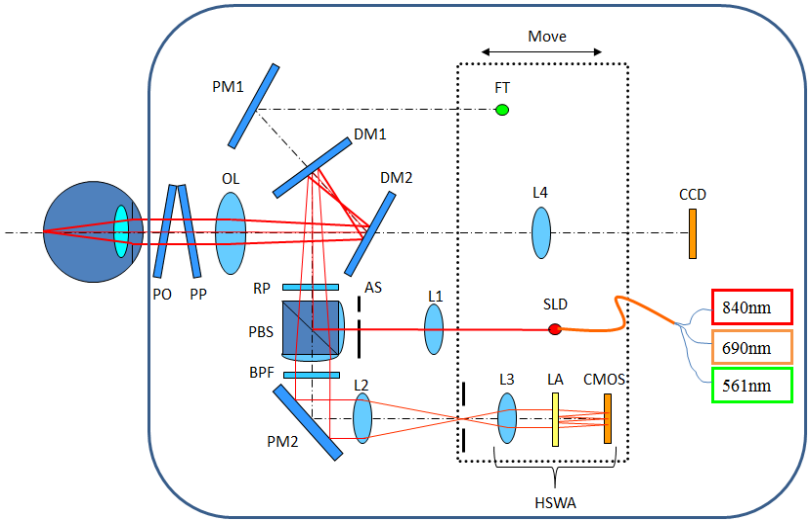

Fig. 1. Schema of the HSWA used. PO is the λ/4 polarizer; PP is the plane plate for the shifting optical axis, OL is the objective lens, DM1 and DM2 are dichroic mirrors; PM1 and PM2 are plane mirrors; RP is the rotation prism; PBS is the polarizing beam splitter, BPF is the bandpass filter; L1–L4 are the lenses, LA is the lens array, AS is the shifted aperture stop, SLD is the superluminescent diode, CCD is used for anterior imaging, CMOS is used for wavefront sensing, and FT is the fixation target.

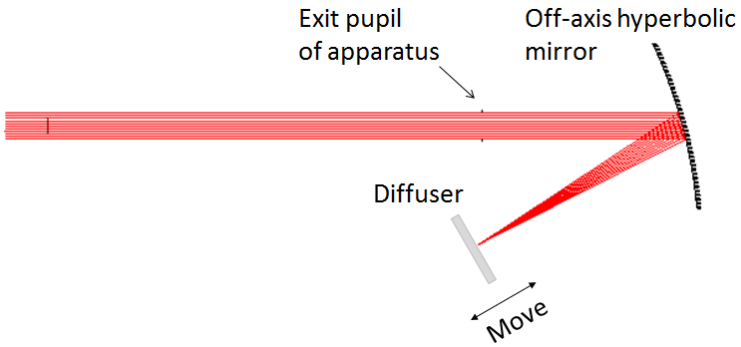

Fig. 2. Layout of reflective artificial eye. The diffuser moves to adjust refraction of the artificial eye from −9 D to 0 D.

2.2 Measurements and statistical analysis

We consecutively measured ocular wavefront aberrations at the three wavelengths by changing the light source every time we measured the aberration. Each sequence, which consisted of three measurements at three wavelengths, took less than a second. The exposure time was 250 ms for 840 nm, 300 ms for 690 nm, and 300 ms for 561 nm. Because the measurements were taken on the natural pupil and an accommodation could be induced during visible-light measurements, we repeated the measurements three to five times for each eye. The operator observed the subject's pupil and waited for restoration of its original size before each successive measurement. As the target was fogged like an auto-refractometer before measurement, the focusing point of subject was the *far point* in the measurement.

Wavefront aberrations were analyzed with a 4-mm-diameter pupil and fitted with up to sixth-order Zernike polynomials. The OSA convention was used for the ordering and normalization of Zernike coefficients [34]. For each wavelength, SE in D was calculated from

#237205 Received 30 Mar 2015; revised 16 Jun 2015; accepted 17 Jun 2015; published 25 Jun 2015

the second-order Zernike defocus coefficient (C_2^0) in microns using Eq. (1) and an amount of adjustment to a focus mechanism in the HSWA.

$$SE = -\frac{4\sqrt{3}C_2^0}{r^2}, \tag{1}$$

where C_2^0 is the Zernike defocus and r is the pupil radius [35]. The methods of fitting a wavefront with Zernike polynomials for least-squares fitting or paraxial curvature matching were explained by L. N. Thibos et al. [35]. In the present study, we used Eq. (1) with Zernike polynomial expansion and least-squares fitting to determine the SE. The LCA was defined as the difference in SEs between two wavelengths, which is the same as Atchison's definition [36]. We calculated the LCA between 840 and 690 nm ($LCA_{840\text{-}690}$), between 690 and 561 nm ($LCA_{690\text{-}561}$), and between 840 and 561 nm ($LCA_{840\text{-}561}$).

For all eyes, we also measured the objective refraction and the biometry of the anterior part of the eye. The SE and power of the cornea (KRT) were measured with an autorefracto-keratometer (KR-1, TOPCON, Japan). The axial lengths (ALs) were measured with an instrument based on low-coherence interferometry (IOLMaster, Carl Zeiss, Germany). For 37 of the 45 eyes, we also obtained the anterior chamber depth (ACD) using an instrument based on a slit-projection method (IOLMaster, Carl Zeiss, Germany). The SE and KRT measurements were repeated thrice, and the AL and ACD measurements were repeated five times. Their averages were used in statistical analyses. We performed a single regression analysis in which the dependent variable was the LCA and the explanatory variable was either age or SE. We also performed Pearson's correlation and partial correlation analyses [37] for all combinations of two variables. We checked whether the slope of the regression was statistically significant and whether the LCA had strong correlations with some variables (statistical analyses; R version 3.0.2 [38]). Pearson's correlation coefficient, for two variables x and y, is

$$r(xy) = \frac{\sum_{i=1}^{N}(x_i - \bar{x})(y_i - \bar{y})}{\sqrt{\sum_{i=1}^{N}(x_i - \bar{x})^2}\sqrt{\sum_{i=1}^{N}(y_i - \bar{y})^2}} = \frac{S_{xy}}{\sqrt{S_x}\sqrt{S_y}}. \tag{2}$$

The partial correlation coefficient between x and y, under the condition that k_1 is a permanent variable, is

$$r(xy \cdot k_1) = \frac{r(xy) - r(xk_1)r(yk_1)}{\sqrt{1-\{r(xk_1)\}^2}\sqrt{1-\{r(yk_1)\}^2}}. \tag{3}$$

The partial correlation coefficient was calculated using the elements of the inverse matrix of Pearson's correlation coefficient matrix for all variables. When the elements of the inverse matrix are expressed as r^{ij}, the partial correlation coefficient between x and y, under the condition that the other variables **k** are permanent variables, is

$$r(xy \cdot \mathbf{k}) = \frac{-r^{xy}}{\sqrt{r^{xx}r^{yy}}}. \tag{4}$$

We evaluated partial correlation coefficients to assess the relationship between the LCA and one other variable at a time, excluding the effects of the remaining variables.

To assess chromatic dispersion, we performed nonlinear regression analysis. Cauchy's equation for the chromatic dispersion of refractive indices is

#237205 Received 30 Mar 2015; revised 16 Jun 2015; accepted 17 Jun 2015; published 25 Jun 2015

$$n(\lambda) = A + \frac{B}{\lambda^2} + \frac{C}{\lambda^4} + \frac{D}{\lambda^6}. \quad (5)$$

Atchison and Smith [36] expanded Cauchy's equation from the refractive index to the SE and fitted the data using Eq. (6),

$$SE(\lambda) = A + \frac{B}{\lambda^2} + \frac{C}{\lambda^4} + \frac{D}{\lambda^6}. \quad (6)$$

They also fitted the chromatic dispersion with Cornu's dispersion equation and Herzberger's equation. They reported that both Cauchy's equation and Cornu's equation were useful guides up to at least 900 nm. Furthermore, they stated that Cauchy's equation ought to be reliable because it is theoretically supported and fits the data well. In the present case, we fitted individual SEs at the three wavelengths in advance using Eq. (7),

$$SE(\lambda) = A + \frac{B}{\lambda^2} + \frac{C}{\lambda^4}, \quad (7)$$

and all data were offset at 590 nm. After that, we fitted all offset data to Eq. (6) and calculated the 95% confidence intervals (CI). Then we compared our results with Atchison's fitting result.

We also fitted our offset data using Cornu's equation and compared the results with the Indiana model eye [14] and Atchison's result. Cornu's equation is

$$SE(\lambda) = p - \frac{q}{\lambda - c}, \quad (8)$$

where p, q, and c are constants.

3. Results

3.1 Biometry and data

Table 1 shows the biometrics and the data. The data given are the averages of the repeated measurements. The KRTs are the averages of the major and minor meridians in diopters.

#237205 Received 30 Mar 2015; revised 16 Jun 2015; accepted 17 Jun 2015; published 25 Jun 2015

Table 1. Biometrics and data from all subjects (G: gender; m; male; f; female).

No.	G	$LCA_{840\text{-}690}$ (D)	$LCA_{690\text{-}561}$ (D)	$LCA_{840\text{-}561}$ (D)	Age (years)	SE (D)	AL (mm)	KRT (D)	ACD (mm)
1	m	0.39	0.57	0.95	22	–6.55	27.32	42.48	4.16
2	f	0.36	0.65	1.02	22	–1.13	23.57	44.12	3.53
3	f	0.32	0.55	0.87	22	–2.83	24.75	44.06	3.79
4	f	0.44	0.48	0.92	22	–4.93	25.34	43.66	3.58
5	f	0.39	0.52	0.91	22	–0.39	22.84	43.69	3.29
6	m	0.36	0.51	0.87	22	–3.83	26.00	42.13	2.83
7	m	0.23	0.67	0.90	22	–3.32	25.64	42.03	3.73
8	m	0.30	0.55	0.86	23	–4.66	26.39	42.56	3.89
9	f	0.38	0.60	0.98	23	–0.70	23.91	44.64	3.73
10	f	0.35	0.64	0.99	24	–3.00	23.65	47.20	—
11	f	0.36	0.63	0.99	25	–2.55	24.62	44.38	3.66
12	f	0.37	0.52	0.89	26	–6.01	27.23	42.45	2.58
13	m	0.38	0.66	1.04	26	–6.60	25.97	44.12	3.69
14	m	0.35	0.66	1.01	28	–1.21	24.76	42.19	2.39
15	f	0.39	0.53	0.92	28	–5.69	25.61	43.86	—
16	m	0.50	0.55	1.05	28	–6.54	26.93	42.35	4.07
17	f	0.39	0.61	1.00	29	–6.59	25.52	43.86	—
18	m	0.34	0.61	0.95	29	–0.99	24.56	42.67	3.62
19	f	0.40	0.55	0.95	29	–5.48	26.35	41.87	3.82
20	m	0.38	0.68	1.06	30	–4.05	25.69	43.21	3.81
21	m	0.40	0.62	1.01	30	–4.05	26.09	42.13	3.90
22	m	0.38	0.69	1.07	30	–1.48	23.72	44.12	3.61
23	m	0.41	0.53	0.94	31	–1.51	24.34	42.00	3.41
24	f	0.33	0.73	1.06	32	–3.83	24.16	45.21	—
25	m	0.31	0.58	0.89	33	–8.25	29.09	41.13	—
26	m	0.38	0.59	0.97	36	–5.17	25.77	42.88	3.45
27	f	0.41	0.55	0.96	41	–0.22	23.56	42.97	3.17
28	f	0.38	0.50	0.88	42	–1.36	23.47	45.18	3.62
29	f	0.41	0.48	0.89	42	–4.49	24.95	43.89	—
30	f	0.39	0.65	1.04	43	–5.03	25.75	44.00	3.27
31	f	0.31	0.70	1.02	44	–1.16	23.81	42.61	—
32	m	0.35	0.58	0.92	44	–1.49	23.84	44.26	3.31
33	m	0.39	0.54	0.93	44	–6.13	26.40	41.54	3.08
34	f	0.32	0.57	0.89	47	–0.71	24.74	42.94	3.71
35	f	0.39	0.63	1.02	47	–4.60	25.80	42.80	1.79
36	f	0.42	0.59	1.01	48	–5.80	25.29	44.85	3.68
37	m	0.39	0.48	0.87	48	–5.68	28.40	39.43	3.42
38	f	0.35	0.65	1.00	49	–6.73	26.36	43.30	3.36
39	m	0.43	0.47	0.91	50	–0.84	23.25	45.24	3.16
40	m	0.37	0.72	1.09	51	–2.78	24.54	43.77	3.15
41	m	0.44	0.55	0.98	52	–6.76	27.22	43.52	—
42	m	0.36	0.53	0.89	53	–4.74	26.00	43.21	3.58
43	m	0.31	0.65	0.96	54	–2.95	25.72	44.76	4.54
44	f	0.34	0.70	1.04	55	–4.80	24.56	45.27	3.44
45	f	0.38	0.62	0.99	57	–1.10	23.14	45.52	3.02

3.2 Precision of measurements

The refraction and chromatic aberrations of the apparatus were calibrated using the reflective artificial eye. The SE calibration errors were less than 0.01 D in the range from –9.0 to 0 D for all wavelengths. Because all of the subjects were Japanese, we expected that most of subjects would be emmetropic and myopic. In fact, all of them were emmetropic and myopic, and the range of the calibration was thus sufficient for this study.

#237205 Received 30 Mar 2015; revised 16 Jun 2015; accepted 17 Jun 2015; published 25 Jun 2015

Figure 3 shows the standard deviations (SD) of the measurements at each wavelength repeated from three to five times for each eye. The average SDs for 840, 690, and 561 nm were 0.085, 0.092, and 0.102 D, respectively. We repeated the measurements four times. The 95% CIs were calculated with the average *m* and the standard error on the assumption that the measurements would vary according to a normal distribution. The expressions for the lower and upper 95% CIs are given by

$$\text{standard error} = \frac{mean\ SD}{\sqrt{n}} = \frac{mean\ SD}{\sqrt{4}}, \tag{9}$$

$$\mu_{Lower} = m - t_{(\varphi,\alpha)} \times \text{standard error} = m - 3.1825 \times \text{standard error, and} \tag{10}$$

$$\mu_{Upper} = m + t_{(\varphi,\alpha)} \times \text{standard error} = m + 3.1825 \times \text{standard error.} \tag{11}$$

The width of 95% CIs for 840, 690, and 561 nm were estimated to be ± 0.13, ± 0.15, and ± 0.16 D, respectively.

We also calculated the LCA for each sequence and evaluated the SD of the LCA for each eye. The results are shown in Fig. 4. The average SDs of the individual LCA for $LCA_{840\text{-}690}$, $LCA_{690\text{-}561}$, and $LCA_{840\text{-}561}$ were 0.052, 0.066, and 0.079 D, respectively. Similarly, the widths of the 95% CIs were estimated to be ± 0.08, ± 0.11, and ± 0.13 D, respectively. Figure 5 shows the results for an eye with the largest SD and the results for an eye with a relatively small SD. For the eye with the largest SD, the fluctuations in measurement between one sequence and the next were large; we judged that these results were strongly affected by the myopic reaction induced by the visible measurements. However, we can speculate that the refractions varied in one sequence less in all the other measurements; that is, we could precisely evaluate the LCA under the natural pupil and free accommodation because we performed one sequence of measurements in a very short time and we repeated sequences.

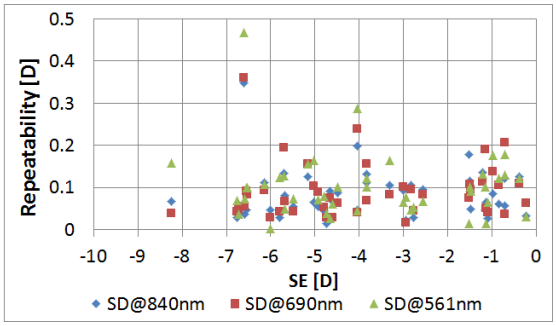

Fig. 3. Standard deviations of SEs within subjects.

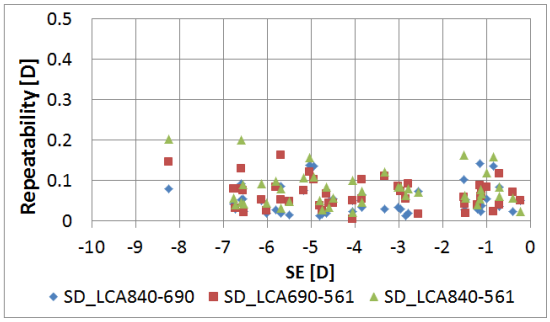

Fig. 4. Standard deviations of LCA within subjects.

#237205 Received 30 Mar 2015; revised 16 Jun 2015; accepted 17 Jun 2015; published 25 Jun 2015

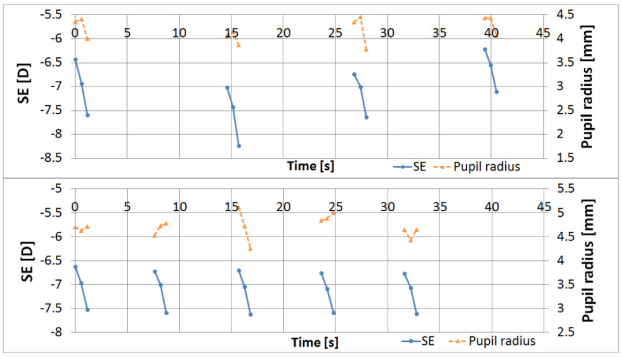

Fig. 5. Circles are SEs for each wavelength. Each solid lines indicates one sequence. The circles in each sequence give the SE of 840, 690, and 561 nm from left to right. Triangles and dotted lines are pupil diameters over time. The top panel shows the results for an eye that had the largest SD among all the subjects. The bottom panel shows the results for an eye that had a relatively small SD.

3.3 Correlations between LCA and other variables

Figure 6 shows plots of the LCA as a function of age for all subjects. We performed simple linear regression analyses. The slopes of the resulting regression lines were approximately 0 and were not statistically significant ($p > 0.05$), although the LCA did increase slightly with age. These results are identical to those of previous studies [24, 25]. Figure 7 shows plots of the LCA as a function of SE for all subjects. The slopes of these regression lines are also not statistically significant ($p > 0.05$).

Pearson's correlation coefficients and the partial correlation coefficients for age, SE, AL, KRT, ACD, and $LCA_{840\text{-}561}$ are shown in Table 2. The upper-right triangle matrix in Table 2 shows Pearson's correlation coefficients, and the lower-left triangle matrix shows partial correlation coefficients. Even though all the Pearson's correlation coefficients and partial correlation coefficients between $LCA_{840\text{-}561}$ and other variables were not large, the Pearson's correlation coefficient between $LCA_{840\text{-}561}$ and KRT was slightly larger than the other Pearson's correlation coefficients for $LCA_{840\text{-}561}$. However, we assumed that an individual LCA was independent of an individual KRT because the partial correlation coefficient between the LCA and KRT was very small. The SE had negative Pearson's and partial correlations with AL. This is reasonable because myopic refraction increases as AL becomes longer. Between SE and KRT, however, the Pearson's correlation was positive but the partial correlation was negative. As KRT, defined as the power of the cornea, grows larger, the total refraction should become more myopic. The partial correlation between KRT and SE is thus reasonable. The Pearson's correlation had the opposite sign, which is also reasonable because KRT and AL have a strong negative correlation and myopic refraction increases as AL becomes longer. This is known as the *small-eye effect*.

#237205 Received 30 Mar 2015; revised 16 Jun 2015; accepted 17 Jun 2015; published 25 Jun 2015

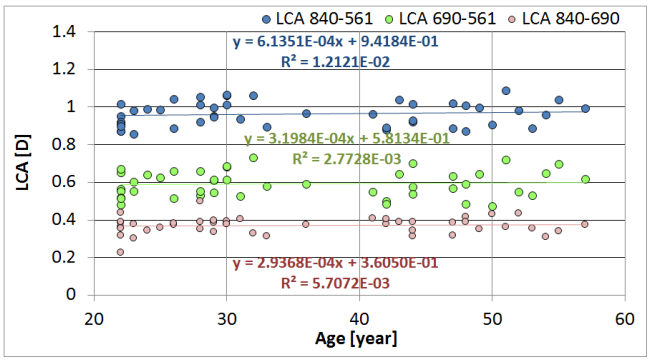

Fig. 6. Average LCA as functions of age.

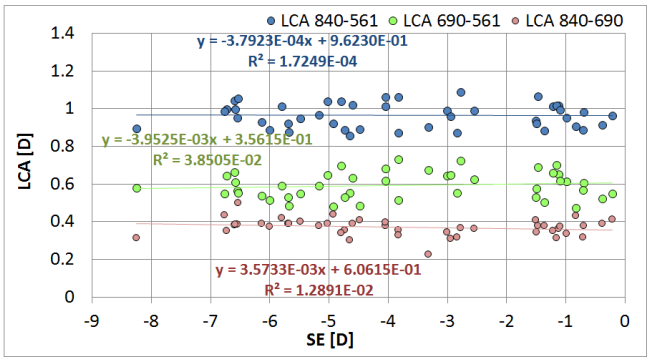

Fig. 7. Average LCA as functions of SE.

Table 2. Correlation coefficients between pairs of variables. Pearson's correlation coefficients are in the upper triangular matrix, and partial correlation coefficients are in the lower triangular matrix.

	$LCA_{840\text{-}561}$	Age	SE	AL	KRT	ACD
$LCA_{840\text{-}561}$		0.130	–0.104	–0.111	0.281	–0.028
Age	0.049		–0.006	–0.080	0.267	–0.174
SE	–0.277	0.116		–0.858	0.351	–0.100
AL	–0.198	0.194	–0.906		–0.678	0.117
KRT	0.048	0.337	–0.595	–0.784		0.121
ACD	–0.024	–0.282	0.226	0.338	0.410	

3.4 Chromatic dispersion between visible and NIR

Figure 8 shows the averages and standard deviations of our results, the individual fittings to Cauchy's equation for each data set, and the fitting to Cauchy's equation using the average data. Each regression was offset at 590 nm in order to compare the results with those of Atchison and Smith [36]. The average and the standard deviation of $LCA_{840\text{-}561}$ were 0.96 D and 0.06 D. Therefore, the 95% CI was 0.96 ± 0.02 D, according to Eqs. (9)–(11) and our number of subjects. Figure 9 shows the results of our regression and of Atchison's regression with Cauchy's equation; the regressions are shown as solid lines, with dashed lines for extrapolates. Atchison and Smith [36] used the data of G. Wald et al., R. E. Bedford et al., and L. N. Thibos et al. [1, 13, 14] for regression with Cauchy's equation, Cornu's equation, and Herzberger's equation in the visible region. They also extrapolated into the near-infrared region and compared their results with the earlier results of N. López-Gil et al., L. Llorente et al., and E. J. Fernández et al. [16, 39, 40]. They reported that the Cauchy and Cornu equations were useful guides for refraction correction from the visible through to the NIR, up to at least 900 nm. For this reason, we used Cauchy's and Cornu's equations to compare the results.

#237205 Received 30 Mar 2015; revised 16 Jun 2015; accepted 17 Jun 2015; published 25 Jun 2015

Figure 10 shows the results of our regression, Atchison's regression, and the Indiana model eye's regression [14] with Cornu's equation. Again, the regressions are shown as solid lines, with dashed lines for extrapolates. Tables 3 and 4 show the coefficients of regression with Cauchy's equation and Cornu's equation, respectively. We modified the Atchison's coefficients for Cornu's equation because the regression showed some bias at 590 nm when we used the coefficients as they were given in the literature. The modified coefficients were shown in Table 4; we changed only the *p* value of Cornu's equation. We also thought it would be useful to compare our results with the earlier results of Fernández et al. [40] using an HSWA, because their data were obtained at many wavelengths between 700 to 900 nm, even though they had only four subjects. The results of Fernández et al. were also used for comparison by Atchison et al. Because the later results of Fernández et al. with seven young adult subjects might have been more accurate, we plotted both the earlier and later data sets [29, 40] in Figs. 9 and 10. Both results were offset to fit our regression at 632.8 nm and 700 nm, respectively.

We applied the coefficients from Table 3 to Eq. (6) and calculated the LCA between 546.1 and 840 nm to be 1.07 D and 0.98 D, for our own results and Atchison's results respectively. We applied the coefficients from Table 4 to Eq. (8) and calculated the LCA between 546.1 and 840 nm to be 1.07, 0.91, and 0.90 D, for our own regression, Atchison's regression, and Indiana's regression, respectively. Our LCA result was larger than either Atchison's or Indiana's. In the case of the regression with Cauchy's equation, in which the difference between our results and Atchison's was smaller than with Cornu's equation, the difference between our regression and Atchison's at 840 nm was lower than the SD of our data (Fig. 9). However, the difference was larger than the 95% CI for our regression. This implies that the chromatic dispersion from our data was larger than that from Atchison's. However, our results showed a tendency similar to that of the later results of Fernández et al. [29]. They reported that there are two possible factors for the discrepancies in the LCA: Atchison's parameters might have been slightly different, and the penetration could be deeper at longer wavelengths. We cannot explain the discrepancy; however, our data do support the later results of Fernández et al. [29], which show a larger LCA than either Atchison or the earlier results of Fernández et al. [40].

We also compared some previous measurements of the LCA; the LCA was 0.72 D between 543 and 788 nm [16], 0.75 D between 532 and 694 nm [28], 0.48 D between 632.8 and 780 nm [29], and 0.55 D between 555 and 700 nm [18]. These tests had 11, 3, 7, and 5 subjects, respectively. The average age and standard deviation were 23 ± 1.5, 26 ± 5.3, 33 ± 3.2, and 29 ± 1.9, respectively. All measurements were performed with HSWA. When we applied the coefficients from Table 3 to Eq. (6), our results were 0.98, 0.81, 0.47, and 0.66 D, respectively, corresponding to each spectral range. Our own results were in good agreement with some of those; however, there were some discrepancies with others. The LCA between 450 and 650 nm was shown in one study [41] using a spatially resolved refractometer, but we did not compare our results with this study because the shortest wavelength of the spectral range was more than 100 nm shorter than our measurements.

#237205 Received 30 Mar 2015; revised 16 Jun 2015; accepted 17 Jun 2015; published 25 Jun 2015

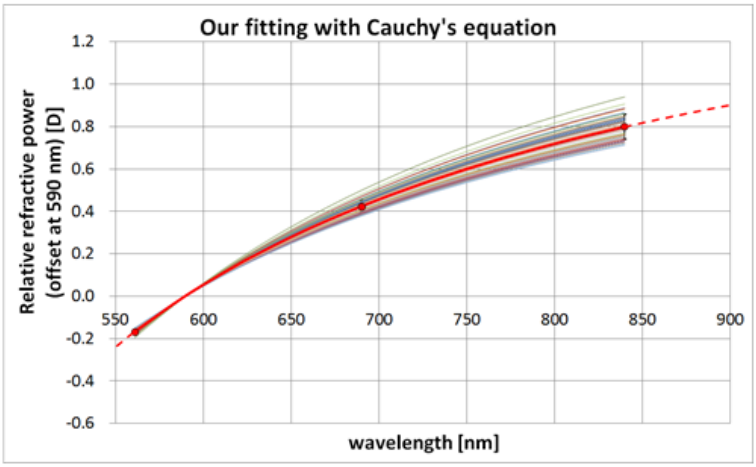

Fig. 8. Regressions to Cauchy's equation for our individual data (solid lines), all data (red line) and its extrapolate (red dashed line). All regressions were offset at 590 nm. Average and standard deviations of our data (red circles and black bars).

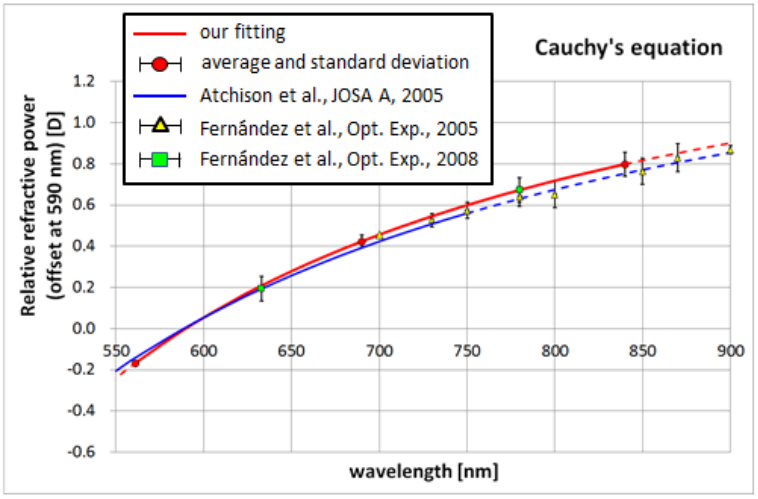

Fig. 9. Regression with Cauchy's equation for our data (red solid line) and its extrapolate (red dashed line). Average and standard deviations of our data (red circles and black bars). Atchison's regression with Cauchy's equation [36] (blue solid line) and extrapolation part (blue dashed line). Average and standard deviation of earlier or later Fernández et al. [29, 40] (green squares, yellow triangles, and black bars). Data sets were offset to match our fitting at 632.8 nm and 700 nm, respectively.

Table 3. Coefficients of regressions for Cauchy's equation.

	A	B	C	D
Our results	1.63814	-6.40514×10^{5}	$+4.32938 \times 10^{10}$	-6.46165×10^{15}
Atchison et al.	1.60911	-6.70941×10^{5}	$+5.55334 \times 10^{10}$	-5.59998×10^{15}

#237205 Received 30 Mar 2015; revised 16 Jun 2015; accepted 17 Jun 2015; published 25 Jun 2015

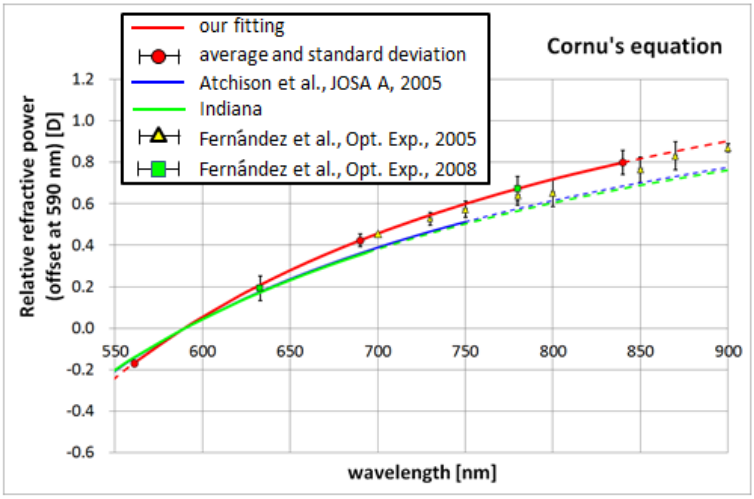

Fig. 10. Regression with Cornu's equation for our data (red solid line) and its extrapolate (red dashed line). Average and standard deviations of our data (red circles and black bars). Atchison's regression with Cornu's equation [36] (blue solid line) and its extrapolate (blue dashed line). Atchison's regression was offset at 590 nm, at which point the value equals zero. Indiana's regression with Cornu's equation [14] (green solid line) and its extrapolate (green dashed line). Average and standard deviation of earlier or later Fernández et al. [29, 40] (green squares, yellow triangles, and black bars). Data sets were offset to match our fitting at 632.8 nm and 700 nm, respectively.

Table 4. Coefficients of regressions for Cornu's equation. The coefficient *p* of Atchison was modified to be offset at 590 nm, at which point the value is zero.

	p	q	c
Our results	1.95821	711.55	226.233
Atchison et al. modified (JOSA A, 2005)	1.70398	633.27	218.358
Indiana model eye (App. Opt., 1992)	1.68524	633.46	214.102

3.5 Higher-order aberrations for the NIR

We considered the relationship between HOA and age because it seemed to be generally thought that HOA increased over time. Figure 11 shows the RMS of individual HOAs for the NIR light source, 840 nm. The HOAs involved here range from third- to sixth-order aberrations. The analyzed pupil size was 4 mm. We performed regression analysis; the slope of the resulting regression line was approximately 0 and not statistically significant ($p > 0.05$).

#237205 Received 30 Mar 2015; revised 16 Jun 2015; accepted 17 Jun 2015; published 25 Jun 2015

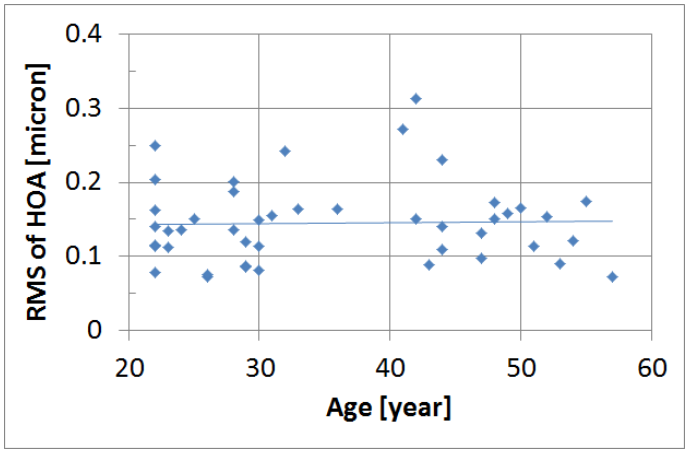

Fig. 11. RMS of HOA for our results as a function of age, and the regression line (solid blue).

4. Discussion

Our results for LCA and age are consistent with previous studies [24, 25]: the LCA did not depend on age. We also found that the LCA between 546.1 and 840 nm was 1.07 ± 0.06 D (average ± SD). The LCA differences between our results and previous results are shown in Table 5. Our results agreed well with two cases [28, 29], and agreed more loosely with two others [18, 40]. It was significantly larger than the results of [16]; the differences were more than 2 SD beyond our results. These differences were significant. We also found that the LCA did not depend on age in the region between the center of visual sensitivity and the NIR among people between 22 and 57 years old. This remains a somewhat unconvincing result because presbyopia is expected to at last develop, along with some chemical changes, in the crystalline lens within the age range of our subjects. However, given the SD LCA result and Fig. 8, individual differences in LCA may be small enough in practical application, because there is only a 0.2 D difference between maximum and minimum from the center of the visible spectrum to the NIR.

Table 5. Comparisons between previous LCA results and our own, corresponding to each comparable spectral regions. Our results were calculated by our coefficients of Cauchy's equation.

	Manzanera et al. [28]	Fernández et al. [29]	Vinas et al. [18]	Fernández et al. [40]	Llorente et al. [16]
Comparable spectral regions [nm]	532~694 nm	632.8~780 nm	555~700 nm	700~850 nm	543~787 nm
Previous results Number of subjects [eye] Range of age [year old] LCA [D]	3 eyes 22~32 yo 0.75 D	7 eyes 27~37 yo 0.48 D	5 eyes 28.6 ± 1.89 yo 0.55 D	4 eyes 27~38 yo 0.31 D	36 eyes (11 eyes with HSWA) 20~71 yo 0.72 D
LCA using our Cauchy's coefficients [D]	0.81 D	0.47 D	0.66 D	0.36 D	0.98 D
Method	All measurements were performed by an HSWA except for Llorente et al.; they used both an HSWA and a laser ray tracing.				

We anticipated that the partial correlation coefficients would reveal whether the LCA is related to the other variables. On the basis of our statistical analyses, however, we find that the geometric ocular parameters such as AL, KRT, and ACD have only weak correlations with the LCA. This suggests that the LCA does not depend on these parameters. We

#237205 Received 30 Mar 2015; revised 16 Jun 2015; accepted 17 Jun 2015; published 25 Jun 2015

performed optical simulation using the CODE V. We used the LeGrand schematic eye [41], which involves chromatic dispersion of the refractive indices of ocular materials and the shapes of all refractive surfaces, and with the aging parameters of Koretz et al. [42]. Measured data, KRT, ACD, and AL, replaced the parameters of the schematic eye. The posterior curvature of the cornea was modified according to the measured anterior curvature so as to retain the ratio between anterior and posterior curvatures of the cornea of LeGrand. The lens thickness, anterior lens curvature, and posterior lens curvature of LeGrand were modified according to Koretz's parameters, using the ages of the subjects. However, we did not duplicate the individual LCA and refraction, precisely because we could not find strong correlation between the geometric data on the LCA or did not measure the individual chromatic dispersion data of the ocular materials. If we acquired such data, we could obtain a valid model of the eye. It may be that the LCA is related to the shape of the crystalline lens, because the effective refractive index of the lens would change with accommodation by changing its curvature, as proposed by Navarro et al. [6]. They focused on the relationship between the effective refractive index and the structure of a gradient index lens.

Collagen in the cornea and crystalline matter in the lens change throughout the age range of our subjects [43, 44]. Given our result, that LCA is unchanged with age, we speculate that the chromatic dispersion of the cornea and lens are small. Although some researchers have reported the refractive indices of the lens at different wavelengths, mostly for animals [45], we could not find any reports on changes in chromatic dispersion with age. Changes with respect to age in the refractive index for a single wavelength were reported in several studies. Dubbelman and Heijde [46] stated that the equivalent refractive index of the crystalline lens decreased at a rate of 0.00039 a year, using a method with a Scheimpflug camera. This implies that the difference in the refractive index between 22 and 57 years is 0.014. Atchison et al. [47] reported a similar decrease in the refractive index, on the basis of analyzing Purkinje images. Using magnetic resonance imaging (MRI), Atchison [47] measured the distribution of the refractive index in the lens and the decrease in the refractive index of the lens nucleus. These data offer a compelling explanation for the lens paradox [48, 49]. It was already known that the curvature of the crystalline lens sharpens with age and that the spherical power of the eye does not increase. This was the lens paradox, and it was solved experimentally with the discovery that the refractive index of the lens decreases. Because the amount of change of the refractive index is less than 0.02 over the age range of our subjects, we speculate that the change in the chromatic dispersion is small.

We estimated the chromatic variance from a change in refractive index using a method introduced in Kröger's paper [50]; the method was to estimate the chromatic variance of the refractive index. What we needed were the refractive indices for wavelengths of 546.1 nm and 840 nm and the LCA of subjects at 22 and 57 years, as estimated from the refractive indices. We modified this method slightly for convenience of application. We needed a set of refractive indices in 590 nm, which we had not measured in the study. We used instead the refractive index values measured with an MRI [49]. We applied the refractive indices, converted to appropriate wavelengths, to the LeGrand schematic eye [41], and then used a paraxial ray tracing to obtain the LCA. We used the LeGrand schematic eye because it has details on the refractive index value for each ocular material. The other differences between the Navarro schematic eye [6], which we used elsewhere, and the LeGrand were a slight difference in vitreous depth and the fact that all refractive surfaces of the LeGrand are spherical. Following a simulation with these refractive indices, using a lens design program (CODE V, Synopsys, Inc. CA), we found a 0.1 D negative change in LCA between ages 22 and 57. However, this simulation and result were not adequate because we left out the changes due to aging in the curvature of the refractive surfaces. We incorporated the aging data from Koretz's study [42], and the size of the LCA change with age was reduced because of the increase of crystalline lens power with age. The conclusion of our speculation about the spectral dispersion of the refractive indices of the ocular substances is that it naturally

#237205 Received 30 Mar 2015; revised 16 Jun 2015; accepted 17 Jun 2015; published 25 Jun 2015

decreases, because the normal ocular substance should follow the average equation Kröger introduced. This means that the change depends just on aging of the refractive index, not on the aging process of chromatic dispersion. However, it was reported that the LCA between 440 and 670 nm depends on age [26, 27]. The aging process of chromatic dispersion might be found in the shorter wavelength range between 440 and 561 nm, which we did not investigate in this study.

It may be useful to compare the LCA's lack of dependence on age with the dependence of other measured values, for example the HOA. Because the accuracy of measurements of NIR HOA in our HSWA has been confirmed by previous studies, it would be worthwhile to compare the LCA–aging relationship with the monochromatic HOA–aging relationship. We found no dependence on age within the age range of our study, 22 to 57 years old (Fig. 11). Fujikado et al. [20] reported that the HOA increased with age, but the increase they discerned appeared in ages beyond the late fifties. A flat tendency in the LCA was shown by Artal et al. [19] until the fifties. In the results of Brunette [21], the LCA were almost equal between 20- to 60-year-olds, which is the same as our own results. According to Larsen's [51] and Mutti et al.'s [52] reports on the increase of ACD, AL, and vitreous chamber depth during the teenage years, bigger physical changes occur in the eye during that period than during young adult (ages 21 to 40) or middle age (41 to 60). Changes to the eye in the elderly population (over 61 years) result from many factors, including physical and anatomic changes, and they do affect the increase in aberrations. Kuroda et al. [53] found significant increasing total ocular aberrations for the nuclear or cortical cataract. But according to the results of Brunette et al. [21], the refractive ocular properties change little in the period between ages 20 and 60. There are only some small changes, for example in the asphericity of the cornea or the crystalline lens, or in the sharpening of the lens. With this information, the independence of HOA from age means that local variations in the refractive index of the cornea and lens do not change between ages 22 and 57.

We also discuss whether individual differences in LCA affect high-resolution retinal imaging. Fernandez et al. [54] reported that the Strehl ratio of retinal image deteriorated somewhat when the bandwidth of the light source was wide and the pupil size was large. Given that the human eye has an LCA of more than 2 D in the visible region, Powell et al. [55] and Benny et al. [56] proposed the chromatic compensation triplet lenses to compensate for it. A primary component of these was a specific triplet lens with null-power to compensate for the human eye's LCA. The performance of these lenses was recently being evaluated for integration into the AO optics [57]. The results of our simple simulation of the polychromatic modulation transfer function (MTF) on the retina, in order to estimate the influence of individual differences in LCA, are shown in Figs. 12 and 13. We used the Navarro schematic eye [6], in which we optimized the surfaces for monochromatic aberration-free eyes, and Powell's triplet lens. Figure 12 shows the result of a simulation of an average case of LCA of the eye, + 1.0 D between 546.1 nm and 840 nm. Figure 13 shows another simulation performed with a value of + 1.1 D, because we considered individual differences in LCA. As the standard deviation, SD, of LCA between 546.1 and 840 nm is ± 0.06 D, the maximum individual difference was assumed to be 0.2 D from the range of 2 SD. As we found the degradation of MTF, the individual compensation of LCA was needed, according to the measurement conditions.

#237205 Received 30 Mar 2015; revised 16 Jun 2015; accepted 17 Jun 2015; published 25 Jun 2015

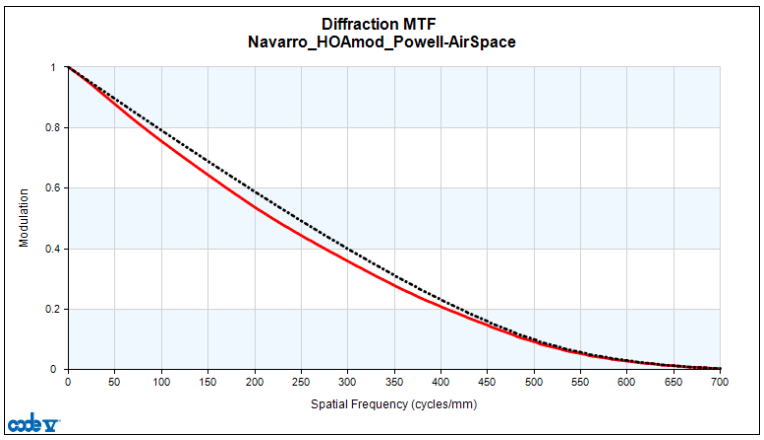

Fig. 12. Polychromatic MTF simulation in which the ocular LCA equals + 1.0 D. Diffraction limit (black line) and simulation result (red line).

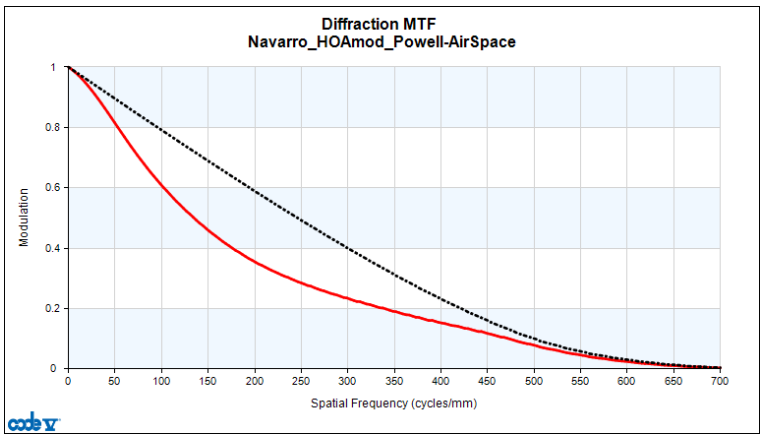

Fig. 13. Polychromatic MTF simulation in which the ocular LCA equals + 1.1 D. Diffraction limit (black line) and simulation result (red line).

Before undertaking this study, we suspected that prescriptions for glasses might be affected by individual differences in LCA. Because the objective refractions were performed in the NIR, the large difference may be an error factor for the objective prescription, although that was small in our results. According to this study, however, the difference is 0.2 D in maximum and minimum, or 0.06 D in SD. In future work, we will apply our instrument for measuring the LCA to an eye with intraocular lenses (IOL), because the LCA is known to be different among different manufacturers [58].

5. Conclusions

We achieved the clinical measurements on scores of subjects using an HSWA systematically. We did not find the LCA to depend on the age of human subjects, 45 eyes, between 22 and 57 years old. The differences of LCA were small among subjects; our results were 1.07 ± 0.06 D (average ± SD) between 546.1 nm and 840 nm. In our future study, we will investigate the LCA in shorter wavelengths and subjects over 60 years old.

Acknowledgments

We are grateful to Tsukuba Hospital personnel and doctors for acquiring data and discussing the results. A part of this research was supported by Topcon Corp.